Proton-Proton Elastic Scattering Involving Large Momentum Transfers*

G. Cocconi,† V. T. Cocconi,† A. D. Krisch,‡ J. Orear,§ R. Rubinstein, D. B. Scarl, and B. T. Ulrich
Laboratory of Nuclear Studies, Cornell University, Ithaca, New York

and

W. F. Baker,§ E. W. Jenkins,|| and A. L. Read
Brookhaven National Laboratory, Upton, New York

(Received 30 November 1964)

Twenty-nine proton-proton differential elastic cross sections for lab momenta p_0 from 11 to 31.8 BeV/c, at four-momentum transfers squared, $-t$, from 2.3 to 24.4 (BeV/c)^2, have been measured at the Brookhaven alternating gradient synchrotron. The circulating proton beam impinged upon a thin CH_2 internal target. Both scattered protons from p-p elastic events were detected by scintillation-counter telescopes which were placed downstream from deflection magnets set at the appropriate angles to the incident beam. The angular correlation of the protons, their momenta, and the coplanarity of the events were determined by the detection system. The results show that at high momentum transfers the differential cross section, $d\sigma/dt$, depends strongly upon the energy; for $-t=10$(BeV/c)^2, the value of $d\sigma/dt$ at $p_0=30$ BeV/c is smaller by a factor$\sim$1000 than at $p_0=10$ BeV/c. At all energies, $d\sigma/dt$ falls rapidly with increasing $|t|$ for scattering angles up to about 65° (c.m.), while in the range from 65 to 90° the cross section falls only by a factor of about 2. The smallest cross section measured was 9×10^{-37} cm^2 sr^{-1}(c.m.), at $p_0=31.8$ BeV/c and $-t=20.4$ (BeV/c)^2; this is about 3×10^{-12} of the zero-degree cross section at the same energy.

1. INTRODUCTION

In recent years, several groups[1,2] have measured differential elastic p-p cross sections at high energies involving four-momentum transfers squared ($-t$) up to 6 (BeV/c)^2. In the present experiment[3] twenty-nine differential elastic p-p cross sections have been measured at the Brookhaven alternating gradient synchrotron (AGS), for lab momenta, p_0, of the incoming proton from 11 to 31.8 BeV/c and for c.m. scattering angles, $\Theta_{c.m.}$, from 30 to 90°. These values correspond to squared four-momentum transfers, $-t=p^2_{c.m.}(1-\cos\Theta_{c.m.})$, from 2.3 to 24.4 (BeV/$c$)^2 and to interaction distances, $\hbar/\sqrt{(-t)}$, from 1.3×10^{-14} to 4×10^{-15} cm.

Section 2 describes the experimental method and Sec. 3 summarizes the results.

2. EXPERIMENTAL METHOD

The experimental layout for a typical measurement is shown[4] in Fig. 1. The circulating proton beam of the AGS was scattered by a thin internal CH_2 target. The scattered and recoil protons, analyzed with respect to angle and momentum by a system of collimators and deflection magnets, were detected by the "left" and "right" counter telescopes, respectively. For each measurement, the deflection magnets D_L, D_{R1}, and D_{R2} were set at the angle and magnetic field strength appropriate for detecting p-p elastic scattering events at the required incident momentum p_0 and angle θ. Proton-proton elastic scattering events were counted by measuring the rate of coincidences between the left and right telescopes. Counting rates for elastic events ranged from about 100 per second for $-t=2.3$ (BeV/c)^2 to about 1 per hour for $-t=24.4$ (BeV/c)^2.

A. Proton Beam

The average intensity of the internal proton beam at the AGS was $\sim10^{11}$ protons per burst, at a repetition rate of 25 bursts per minute. The beam made many traversals through the target. The average total length of target traversed was comparable with the mean free path of the beam protons in CH_2. Thus there were approximately 10^{11} collisions per burst in the target.

The target, initially several inches away from the beam, was rapidly flipped (in about 10 msec) into position, a few mm from the equilibrium orbit of the beam, about 50 msec before the end of the acceleration cycle. A long and uniform spill of the beam onto the target was achieved by turning off the radio-frequency acceleration on reaching the desired momentum p_0 and

* Work done under the auspices of the U. S. Atomic Energy Commission and the National Science Foundation.

† Present address: CERN, Geneva, Switzerland.

‡ Present address: University of Michigan, Ann Arbor, Michigan. National Science Foundation, Predoctoral Fellow.

§ Presently on leave of absence at CERN, Geneva, Switzerland.

|| Presently on leave of absence at University of Arizona, Tucson, Arizona.

[1] A. N. Diddens, E. Lillethun, G. Manning, A. E. Taylor, T. G. Walker, and A. M. Wetherell, *1962 International Conference on High-Energy Physics at CERN* (CERN Scientific Information Service, Geneva, Switzerland), p. 576; W. F. Baker, E. W. Jenkins, A. L. Read, G. Cocconi, V. T. Cocconi, and J. Orear, Phys. Rev. Letters **9**, 221 (1962); K. J. Foley, S. J. Lindenbaum, W. A. Love, S. Ozaki, J. J. Russell, and L. C. L. Yuan, *ibid.* **10**, 376 (1963); **11**, 425 (1963).

[2] For 1 BeV see, for example, J. D. Dowell, W. R. Frisken, G. Martelli, B. Musgrave, H. B. van der Raay, and R. Rubinstein, Nuovo Cimento **18**, 818 (1960); D. Bugg, A. J. Oxley, J. Zoll, J. G. Rushbrooke, V. E. Barnes, J. B. Kinson, W. P. Dodd, G. A. Doran, and L. Riddiford, Phys. Rev. **133**, B1017 (1964). For 2–6 BeV see, for example, B. Cork, W. A. Wenzel, and C. W. Causey, *ibid.* **107**, 859 (1957).

[3] G. Cocconi, V. T. Cocconi, A. D. Krisch, J. Orear, R. Rubinstein, D. B. Scarl, W. F. Baker, E. W. Jenkins, and A. L. Read, Phys. Rev. Letters **11**, 499 (1963). W. F. Baker, E. W. Jenkins, A. L. Read, G. Cocconi, V. T. Cocconi, A. D. Krisch, J. Orear, R. Rubinstein, D. B. Scarl, and B. T. Ulrich, *ibid.* **12**, 132 (1964).

[4] Some additional experimental details are contained in a thesis by A. D. Krisch, Cornell University, 1964 (unpublished).

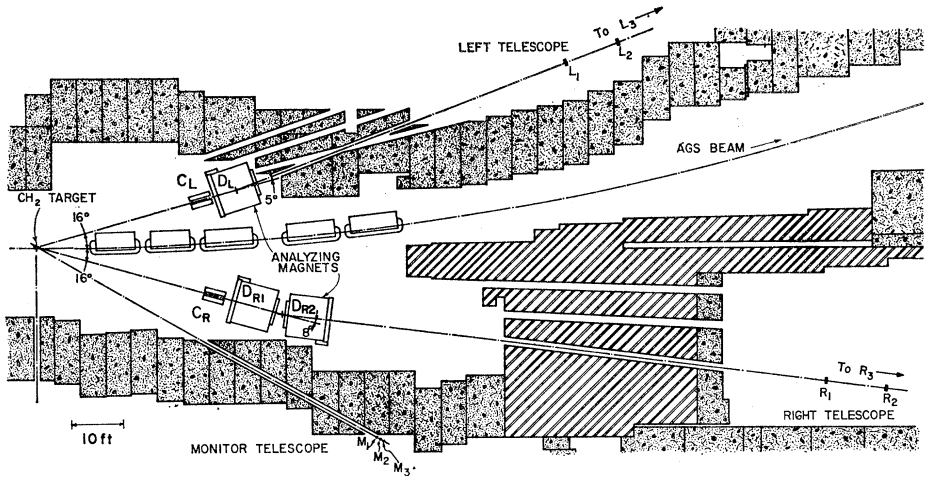

FIG. 1. Experimental layout for one of the measurements. Internal beam momentum $p_0=21.9$ BeV/c and momentum transfer $-t=19.6$ (BeV/c)^2.

holding the field of the AGS magnets essentially constant for approximately 400 msec. A beam spill of duration up to $\approx$300 msec was then obtained as the beam slowly drifted radially onto the target. The uniformity of the spill was improved by using thin targets.

The energy stability of the proton beam was approximately $\pm 0.3\%$, while the absolute energy calibration was correct to within about 1%. The energy loss due to the multiple traversals of the beam through the target was $\approx$0.1 BeV. The accelerated beam energy was consequently always set at 0.05 BeV above the required value of the incident beam energy.

The angular spread of the beam was about 1 mrad, primarily due to the multiple scattering of the circulating beam in the target. The effective beam spot-size, as indicated by the blackening of the target by the beam, was typically a few millimeters in diameter.

B. CH_2 Target

The target protons for the p-p scattering were the hydrogen nuclei in a polyethylene target (density 0.964 gcm^{-3}). The prolonged exposure of the target to the beam resulted in blackening, melting, and cracking of the target material. The hydrogen depletion of the polyethylene was not negligible; in fact, approximately 10% of the hydrogen would be lost in a CH_2 target exposed for about 30 min to the full AGS beam. These problems were particularly severe for the thin targets which were necessary for obtaining a long beam spill. Some of these inconveniences were lessened by constructing special targets[5] consisting of a wheel of polyethylene 1 to 2 mm thick, which was rotated about its axis by approximately 10° between successive beam bursts. As the beam hit the rim of the wheel, the damage was spread over the entire circumference, thereby increasing the useful lifetime of the target from 30 min to about 6 h.

[5] C. R. Flatau (to be published).

Since 1/7 of the nucleons in CH_2 are protons in hydrogen, and 3/7 are protons in carbon nuclei, one might expect that the carbon protons would give a large background due to quasielastic p-p scattering. Pure carbon targets, built exactly like the CH_2 targets, were used to determine the contribution from carbon. As discussed in Sec. F, it was found that in our experiment the quasielastic events represent only about 2% of the recorded events, for most of the cross sections measured.

C. Secondary Beam Analysis

The experimental arrangement for detecting the scattered and recoil protons is shown in Fig. 1. The triple scintillation counter telescopes, $L\equiv L_1L_2L_3$, and $R\equiv R_1R_2R_3$, detected the left- and right-scattered protons, respectively. The solid angle of acceptance for p-p elastic scattering events was defined by one of these six counters (usually either L_2 or R_2); it was typically about 10^{-4} sr in the lab system, corresponding to about 10^{-3} sr in the c.m. system.

The collimators C_L and C_R served to reduce background. Their aperture subtended a solid angle at the target larger than that subtended by the defining counter, in order to eliminate any uncertainties in solid angle caused by effects at the collimator walls.

The deflection magnets D_L, D_{R1}, D_{R2}, served to analyze the momenta of the particles detected by the counters. The angles of deflection α varied from 5 to 30°; the momentum acceptance in a counter telescope was typically $\approx\pm 5\%$. Each magnet was 6 ft long with 18-in.$\times$6-in. aperture. The magnet calibration data given by Danby[6] were compared with nuclear magnetic resonance probe and floating-wire measurements of the magnetic field. All methods agreed to within 1%. The magnets, each weighing 30 tons, were mounted on hydraulic "feet" for maneuvering them rapidly ($\approx$20 ft/h) from one position to another.

[6] G. T. Danby, BNL Accelerator Department Report GTD-2 (unpublished).

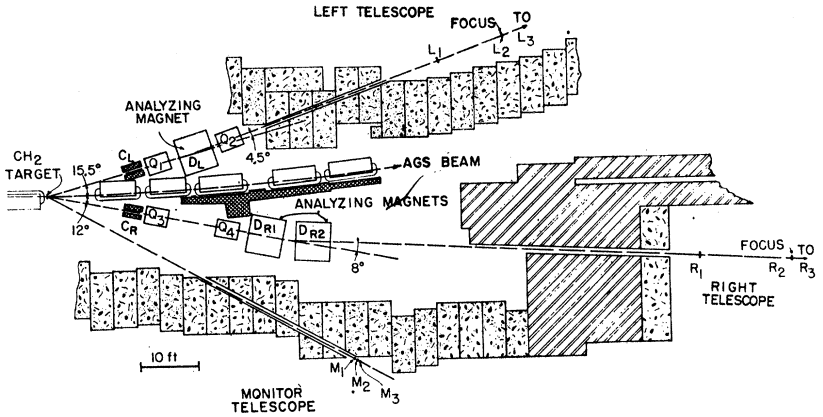

FIG. 2. Experimental layout for one of the measurements using quadrupoles. Internal beam momentum $p_0=30.9$ BeV/c and momentum transfer $-t=24.4$ (BeV/c)^2.

Iron and heavy-concrete shielding walls of thickness up to 44 ft were built, mostly to minimize the background due to muons with energies up to ≈ 20 BeV. For the most difficult measurements, an additional shielding wall of lead bricks, 2 ft thick and 35 ft long, was built right against the AGS vacuum tank. This reduced the background for the R telescope by a factor of 10 to 15.

Each of the beam channels built through the shielding walls was used for several cross section measurements. This was achieved by deflecting the secondary beams towards the AGS ring, and holding constant the final beam direction after the deflection.

An additional reason for deflecting the secondary beams "inward" whenever possible was that this caused a kinematical focusing effect in the horizontal plane which increased the solid angle for p-p elastic scattering events subtended at the CH_2 target by a given counter. This effect is a consequence of the momentum-angle correlation for elastically scattered protons. In fact, for a given incident proton energy, an increasing scattering angle corresponds to a decreasing secondary proton momentum, resulting in a larger angle of deflection for protons at the larger scattering angle. A further advantage derived from deflecting the secondary protons "inward" was that at the telescopes the sensitivity of the angular correlation for p-p elastic events to the value of the incident energy was much smaller than would be the case if the secondary particles were deflected "outward."

For the two cross section measurements at the highest $|t|$ values [$p_0=31.8$ BeV/c, $-t=20.4$ (BeV/c)^2, and $p_0=30.9$ BeV/c, $-t=24.4$ (BeV/c)^2], quadrupole doublet lenses were employed in both secondary beam channels (see Fig. 2). All four quadrupoles were 48 in. long, with 8-in. aperture. The use of quadrupoles and of somewhat smaller counters made it possible to increase the solid angle subtended by either counter telescope by a factor of about 3, i.e., to $\approx 3\times 10^{-3}$ sr (c.m.), while the number of background counts in a telescope was reduced by a factor of about 2. The improvement in the ratio of true coincidences to accidental coincidences between the L and R counter telescopes was thus a factor of about 12. For the two differential cross sections measured using quadrupoles, the rate of p-p elastic scattering events was about 1 to 2 per hour. In these two measurements, one of the collimators (C_R) was made to be the defining aperture for the acceptance solid angle of the system, i.e., the counters used were larger than the calculated spot size. The edges of the collimator aperture did not appear as sharply defined boundaries for high-energy protons; we estimate that the uncertainty in the solid angle due to this fuzziness was $\lesssim 10\%$.

D. Counters and Electronics

Both the L and R counter telescopes consisted of three rectangular plastic scintillators, each of thickness $\frac{1}{2}$ in.; the area of one of these six counters (which varied in size from 5 in.$\times$6 in. to 14 in. $\times$16 in.) determined the acceptance solid angle of the system for p-p elastic scattering events. Usually, the middle counter of one of the telescopes (L_2 or R_2) defined the solid angle ("defining" counter). The other counters were made to subtend a larger solid angle in order to allow for possible errors of $\approx 1\%$ in the beam energy and $\approx 1\%$ in the fields of the deflection magnets, and also to allow for the multiple scattering of the incident beam in the CH_2 target and of the secondary protons along their flight paths (in the window of the target vacuum box, in the air, and in the scintillators). As an example, for a typical cross section measurement, the defining counter L_2 was 12 in. (horizontal)$\times$12 in. (vertical). The R_2 size which corresponded to the same subtended solid angle was 8 in.$\times 5\frac{1}{2}$ in., while the R_2 counter actually used was 12 in.$\times 7\frac{1}{2}$ in.

The scintillators were viewed through $\frac{1}{2}$-in.-thick Lucite light guides by RCA 7746 10-stage photomultiplier tubes, operated at about 2300 V. The risetime of the photomultiplier output pulse was about 2 nsec and the time jitter was $\lesssim 1$ nsec. The anode output pulse of each photomultiplier was fed, through about 150 ft of RG8U cable, into a Chronetics Model 101, 100-Mc/sec transistorized discriminator unit. The dis-

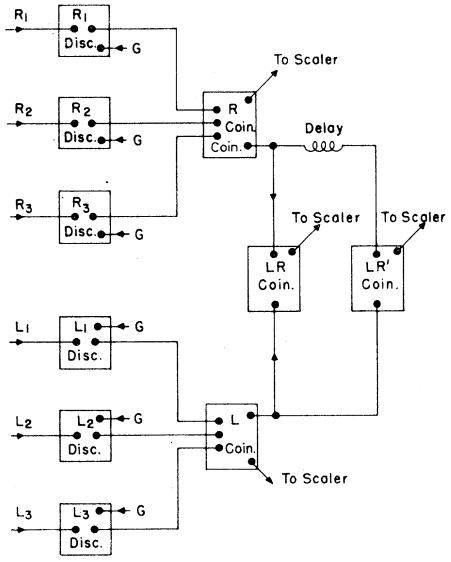

FIG. 3. Block diagram of circuitry for coincidence system. Blocks labeled DISC and COIN are discriminator and coincidence circuits, respectively.

criminators were gated "on" only during that part of the beam spill which was reasonably uniform.

A block diagram of the fast electronic logic is shown in Fig. 3. The pulse widths and coincidence resolving times were determined by shorted stubs. Four quantities were recorded by fast scalers: the coincidences $R \equiv R_1R_2R_3$, i.e., the number of particles passing through the R telescope; $L \equiv L_1L_2L_3$, the number passing through the L telescope; LR= the number of coincidences between L and R telescopes; and LR', a measure of the accidental coincidences between the L and R telescopes, taken with the relative L-R time delay detuned by about 20 nsec. These coincidences all had a resolving time of about 4 nsec.

In the more difficult measurements, the LR' rate turned out to be comparable to the LR rate, indicating that faster resolving time was needed, along with a more accurate method of measuring the background due to accidental coincidences.

The faster resolving time was achieved by observing the L-R time difference spectrum on a multichannel pulse-height analyzer. As shown in Fig. 4, pulses from the L_1 and R_1 discriminators were fed, through a gate circuit (described below), into a Chronetics Model 105 time-to-height converter. The output pulse from this unit was proportional in height to the difference in arrival time of the L_1 and R_1 pulses and was fed into a TMC CN-110 multichannel pulse-height analyzer (PHA). In order to reduce background from L_1 R_1 chance coincidences and to reduce counting losses in the PHA, the output of a slow (50-nsec resolving time) coincidence between the L and R telescopes was used to gate the L_1 and R_1 inputs to the time-to-height converter. A typical PHA display is shown in Fig. 5; the width of each channel corresponds to about 0.5 nsec. The peak, of full width about 2 nsec, contains the true coincidence events. The level of the background in this peak due to accidental coincidences could be determined very precisely by averaging over the remainder of the 50-nsec time base.

A useful feature of the coincidence system using the PHA was that one was only required to estimate the relative L-R time delay correct to within $\approx$20 nsec, in order to be able to detect the p-p elastic events. In the most difficult measurements it would have been impossible to find the exact timing between the L and R telescopes by the standard method of taking an L-R delay curve.

The two systems shown in Figs. 3 and 4 were in use during all 29 measurements. Because of the greater

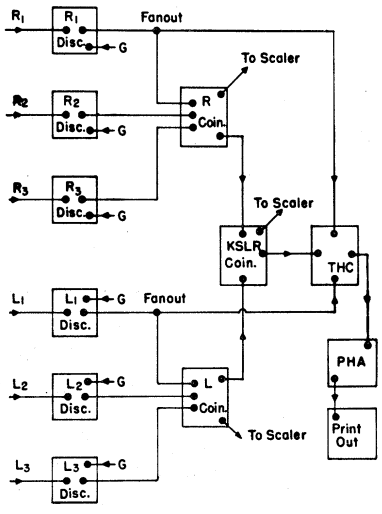

FIG. 4. Block diagram of circuitry for pulse-height analysis system. The KSLR COIN is a 50-nsec coincidence used to gate the time-to-height converter, THC.

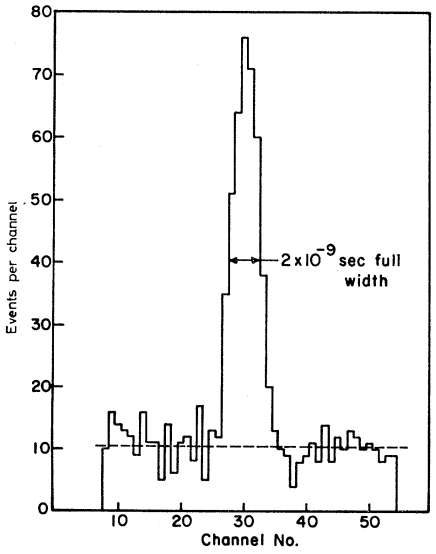

FIG. 5. Typical resolution curve from the pulse-height analyzer. Number of coincidences is plotted against difference in time of arrival of left and right pulses.

accuracy, only data from the pulse-height analyzer system were used to compute the cross sections.

Resolving time was also improved by taking care to reduce the effect of variations in the travel time of light in the scintillators. This was achieved by mounting the counters so that the phototubes of the L telescope were below their scintillators and those of the R telescope were above. When an elastically scattered proton goes through the L telescope above the median plane, because of coplanarity its mate will go through the R telescope below the median plane, and hence the increase in light travel time would be the same for both counters L_1 and R_1. This was confirmed by observing a loss of time resolution of ≈ 2 nsec whenever one counter was turned upside down.

The length of an L or R telescope was typically about 20 ft. However, for some of the measurements in which the ratio of true coincidences to accidental coincidences was particularly low, the length of one or both telescopes was increased up to about 80 ft. It was thus possible to reduce the number of "stray" particles counted by a telescope without reducing the number of detected p-p elastic events. By this means, we could increase the ratio of true to accidental coincidences by as much as a factor ≈ 25.

E. Monitoring Method

To measure absolute cross sections, it was necessary to determine the number of proton traversals through the CH_2 target, corresponding to a measured number of events detected by the coincidence PHA logic system. A scintillation counter telescope, $M_1M_2M_3$ (see Fig. 1) about 2 ft long, using $\frac{1}{8}$-in.-diam scintillators connected to RCA 7746 phototubes via air light guides, provided a relative measure of the number of protons passing through the target. The monitor telescope was calibrated, for each CH_2 target specimen, by analyzing the target for its Be^7 activity, the Be^7 being produced by carbon spallation. The Be^7 nucleus decays by K capture (mean life 77.5 days), followed by the emission of a 0.48-MeV γ ray, with branching ratio $f=0.1032$.[7] The γ activity N_γ of each target was measured with a NaI γ-ray spectrometer, calibrated with a standard γ-ray source. Taking the production cross section for Be^7 to be $\sigma(Be^7)=9.5\pm 0.5$ mb,[8] the total number of protons which passed through the CH_2 target, and hence the absolute differential p-p elastic cross section, can be calculated:

$$\frac{d\sigma}{d\omega}=\frac{1}{\tau}\frac{e^{-t/\tau}}{\epsilon f N_{pp} N_{MT}}\frac{\sigma(Be^7)}{n_H N_M N_\gamma}\frac{}{\Delta\omega},$$

where τ is the Be^7 mean life, N_{pp} is the number of true left-right coincidences in a given run, N_M is the number of M-telescope counts recorded in the same run, N_{MT} is the total count in the M telescope during the exposure of the target, $\epsilon=0.00651$ is the efficiency of the NaI counter for detecting the 0.48-MeV γ rays; the factor $e^{-t/\tau}$ takes into account the decay of Be^7 nuclei during the interval between irradiation and analysis of the target, and $n_H(=2)$ is the ratio of hydrogen nuclei to carbon nuclei. Note that the N_M coincidence counts were gated "on" only during the uniform part of the beam spill, along with the L and R discriminators, while the N_{MT} coincidence system was ungated, in order to record the total number of protons passing through the target during its exposure.

F. Background from Quasielastic and Inelastic Processes

In addition to solving the background problems due to accidental coincidences, it was necessary to demonstrate that the events counted were not due to p-p quasielastic scatterings from the protons in the carbon nuclei, nor to inelastic p-p scatterings, such as for example $p+p\rightarrow p+p+\pi^0$.

The kinematical constraints of our detection system were sufficiently tight to discriminate strongly against quasielastic p-p scattering events. Calculations have shown that we could only detect events for which the target protons, in carbon, lay inside a small ellipsoid of momentum space within the Fermi sphere. For a typical cross section measurement, the three radii of the ellipsoid were $P_1=12$ MeV/c, $P_2=68$ MeV/c, and $P_3=160$ MeV/c. Assuming that the Fermi sphere (radius $P_f=230$ MeV/c) is uniformly populated by carbon protons, then the fraction of these carbon protons which could give detectable events is

$$f\sim\frac{\frac{4}{3}\pi P_1P_2P_3}{\frac{4}{3}\pi P_f{}^3}\simeq 1\%.$$

Because of screening effects in the carbon nucleus and the large probability that a secondary proton may interact with the carbon nucleus a second time before leaving it, the effective ratio of carbon protons to hydrogen protons is probably significantly less than the actual ratio of 3:1. It follows from the above arguments that the expected background in the detected events due to the quasielastic p-p scattering should be $\approx 2\%$.

The quasielastic scattering effect was studied experimentally by measuring LR coincidences with a pure carbon target replacing the CH_2 target. The LR coincidence rate with a carbon target was typically ≈ 1–3% of the rate with a CH_2 target. For most of the measurements, the correction was 2%. However, for the measurements using quadrupoles, where the subtended solid angles and momentum bites became appreciably larger, the carbon subtraction was about 8% of the event rate with a CH_2 target.

Another possible source of background was inelastic

[7] J. G. V. Taylor and S. J. Merrit, Can. J. Phys. **40**, 926 (1962).
[8] J. B. Cummings, J. Hudis, A. M. Poskanzer, and S. Kaufman, Phys. Rev. **128**, 2392 (1962).

proton-proton events. Typical reactions might be:

$$p+p \rightarrow p+p+\pi^0,$$
$$p+p \rightarrow p+n+\pi^+,$$
$$p+p \rightarrow p+p+\pi^+ +\pi^-.$$

Convincing evidence that the inelastic background due to such processes was not significant came from the low event rate in the carbon target runs compared with the CH_2 target runs. A significant inelastic background would almost certainly have been detected in the carbon runs. The Fermi momentum in the carbon nucleus would indeed affect the distribution of the secondary particles from inelastic processes; however, this effect should nevertheless make little difference to the number of inelastic events detected by our system, unless the inelastic differential cross section is peaked in a pathological way. Thus, the fact that no inelastic events were apparently counted using a carbon target (the observed events are attributed, as we have seen, to quasielastic p-p scattering) is strong evidence that the inelastic background was $\lesssim 2\%$.

Another experimental check of the inelastic background level was made by taking cross section measurements with the counter areas in both L and R telescopes decreased by a factor of 2. If the detected events were elastic, then the event rate should decrease by a factor of 2. If, however, we were observing a significant number of inelastic events, then the event rate should decrease by as much as a factor of 4. The event rate fell by a factor of 2, indicating that the events counted were indeed elastic p-p scatterings.

It should be noted that all so-called "elastic scattering" events involve the emission of photons due to bremsstrahlung. Thus, what we mean by an elastic p-p scattering event is the process:

$$p+p \rightarrow p+p+\text{photons}.$$

The emission of a photon with high energy ($\gtrsim 50$ MeV) would destroy the angle and momentum correlation of the two secondary protons. A rough estimate, based on the assumption that the radiative correction for p-p scattering is similar to that for e-e scattering, indicates that $\lesssim 5\%$ of the "elastic" events are not detected because of this effect[9]; a 2% correction was applied to all cross section measurements.

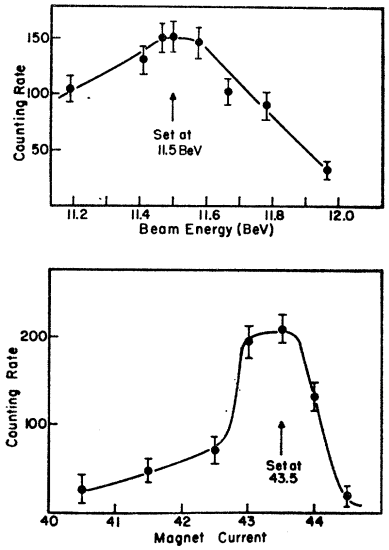

FIG. 6. Beam-energy curve and magnet curve. The upper plot is the number of left-right coincidences as a function of the energy of the incident beam. The lower plot is the number of left-right coincidences as a function of current in one of the analyzing magnets.

G. Experimental Errors

The cross section measurement at $p_0=30.9$ BeV/c, $-t=24.4$ (BeV/c)^2, which had the lowest counting rate (≈ 1 per hour), had 25 events; the statistical error was 25% after subtracting the background. For most of the other measurements the statistical error was less than 10%. However, the over-all systematic error was in general somewhat larger ($\approx 20\%$).

One possible source of systematic errors was the inaccurate alignment or positioning of magnets, collimators, and counters. All such errors would result in the actual solid angle being smaller than the calculated one. The resulting error in the cross section was estimated to be $+10\%$, -0%. In the measurements using quadrupoles, however, this uncertainty in the cross section was estimated as $+40\%$, -15%.

Other systematic errors were due to incorrect values of beam energy and magnetic field strengths, as well as to uncertainties in the focusing properties of the magnets for large angles of deflection. The uncertainty in the calculation of "nominal" solid angles was taken to be $\pm 5\%$, except for the quadrupole system where this uncertainty was $+30\%$, -10%. These errors were minimized by measuring the coincidence counting rate as a function of the beam energy and the field strengths. Typical data from such measurements are shown in Fig. 6. The center of the wide, flat peak of these curves indicated the correct beam energy or field strength; that value was usually in agreement with the calculated value. The coincidence counting rate fell to less than a few percent when the beam energy or one of the magnetic fields was detuned from its correct value; this was good evidence that only events with the correct p_0, P_L, and P_R, corresponding to p-p elastic scattering events, were counted.

Another source of systematic errors was our beam monitoring system. The uncertainty in the Be^7 production cross section is $\pm 5\%$; the branching ratio for the 0.48-MeV γ-ray decay mode is only known to $\pm 8\%$; the uncertainty in the NaI spectrometer calibration was $\pm 3\%$. The calibration of the monitor counter telescope $M_1M_2M_3$ was found to vary slightly during the course of the experiment, probably because at different times the beam spill came from different spatial regions of the target, and part of it, occasionally, from the target holder. The uncertainty in monitor calibration due to this cause was taken to be $\pm 10\%$.

Corrections to the data were made for the number of secondary protons which were lost by scattering in the windows of the CH_2 target vacuum box, in air, and in

[9] J. S. Levinger (private communication).

TABLE I. The twenty-nine p-p elastic cross sections measured in this experiment.

$-t$ (BeV/c)^2	p_0 (BeV/c)	$\Theta_{c.m.}$ (deg)	$(d\sigma/d\omega)_{c.m.}$ (cm^2/sr)	$X=\frac{(d\sigma/d\omega)}{(d\sigma/d\omega)_0}$	Percent error in $d\sigma/d\omega$ and X (%)
2.25[a]	18.9[b]	29.9[c]	1.61×10^{-30}	7.31×10^{-6}	+25, −20
2.28	13.0	37.0	3.06×10^{-30}	2.06×10^{-5}	+25, −20
3.15	11.0	48.1	1.52×10^{-30}	1.22×10^{-5}	+25, −20
3.50	16.1	40.8	5.12×10^{-31}	2.74×10^{-6}	+25, −20
3.80	24.9	33.8	1.16×10^{-31}	3.96×10^{-7}	+25, −20
4.30	13.1	51.5	1.30×10^{-31}	8.77×10^{-7}	+25, −20
4.30	18.1	42.8	7.43×10^{-32}	3.51×10^{-7}	+25, −20
6.00	11.1	68.3	4.02×10^{-32}	3.22×10^{-7}	+25, −20
6.00	15.7	55.4	1.29×10^{-32}	7.04×10^{-8}	+25, −20
6.00	21.7	46.2	5.98×10^{-33}	2.35×10^{-8}	+25, −20
6.00	31.5	37.7	3.53×10^{-33}	9.42×10^{-9}	+25, −20
7.80	12.9	72.1	9.83×10^{-33}	6.68×10^{-8}	+25, −20
7.80	18.2	58.8	2.52×10^{-33}	1.18×10^{-8}	+25, −20
7.80	25.0	49.1	9.78×10^{-34}	3.31×10^{-9}	+25, −20
9.90	11.4	90.0	2.24×10^{-32}	1.74×10^{-7}	+25, −20
10.00	14.2	78.4	5.10×10^{-33}	3.11×10^{-8}	+25, −20
10.00	20.9	62.1	4.84×10^{-34}	1.97×10^{-9}	+25, −20
10.00	28.7	52.0	1.47×10^{-34}	4.30×10^{-10}	+30, −25
11.12	30.7	53.7	4.47×10^{-35}	1.23×10^{-10}	+30, −25
11.56	19.6	70.2	2.82×10^{-34}	1.23×10^{-9}	+30, −25
12.01	16.0	81.4	1.54×10^{-33}	8.30×10^{-9}	+25, −20
12.46	23.8	65.2	8.41×10^{-35}	3.01×10^{-10}	+30, −25
13.94	21.9	73.1	6.90×10^{-35}	2.69×10^{-10}	+30, −25
14.50	18.0	86.0	3.65×10^{-34}	1.74×10^{-9}	+25, −20
15.06	26.6	68.1	1.46×10^{-35}	4.64×10^{-11}	+30, −25
18.77	26.2	77.9	5.18×10^{-36}	1.67×10^{-11}	+35, −30
19.65	21.9	90.0	5.15×10^{-35}	2.00×10^{-10}	+30, −25
20.38	31.8	72.8	9.20×10^{-37}	2.41×10^{-12}	+100, −50
24.39	30.9	82.4	1.10×10^{-36}	3.00×10^{-12}	+100, −50

[a] All squared four-momentum transfers t have an error of ±1%.
[b] All internal beam momenta p_0 have an error of ±1%.
[c] All center-of-mass scattering angles have an error of ±0.2°.

scintillators. While total cross sections for these absorption effects are known, the differential cross sections are not, and it is therefore difficult to estimate the effect of the reactions yielding a charged particle in the forward direction, which may still be counted. It was estimated that (65±20)% of the protons which interacted along their flight path failed to reach the final scintillator (L_3 or R_3). The over-all correction factor for the absorption of protons was taken to be 1.25±0.05.

The uncertainty in the absolute value of incident momentum, p_0, was ±1%, and the uncertainty in the absolute value of scattering angle, ±0.2° (c.m.).

3. RESULTS AND DISCUSSION

The twenty-nine differential elastic p-p cross sections measured are listed in Table I and are plotted as a function of $(-t)$ in Fig. 7. In this graph, the ordinate is the normalized cross section X, defined as

$$X=\left(\frac{d\sigma}{d\omega}\right)_{c.m.}\Big/\left(\frac{d\sigma}{d\omega}\right)_0,$$

where

$$(d\sigma/d\omega)_0=(k\sigma_T/4\pi)^2.$$

The latter equation uses the optical theorem to calculate the zero-degree cross section; σ_T, the total p-p cross section, was taken to be 40 mb.

The cross section is seen to be strongly dependent upon both angle and energy. At a fixed angle, say $\Theta_{c.m.}=90°$, the cross section falls by a factor of 2×10^4, as p_0 is increased from 10 to 30 BeV/c. At a fixed momentum, say $p_0=20$ BeV/c, the cross section falls by a factor of 4×10^4, as $\Theta_{c.m.}$ is increased from 30 to 90°. Note also the following features of the data:

(1) The energy dependence of the cross section, at a fixed momentum transfer, becomes more pronounced the higher the momentum transfer.

(2) At a fixed energy, the cross sections decrease less

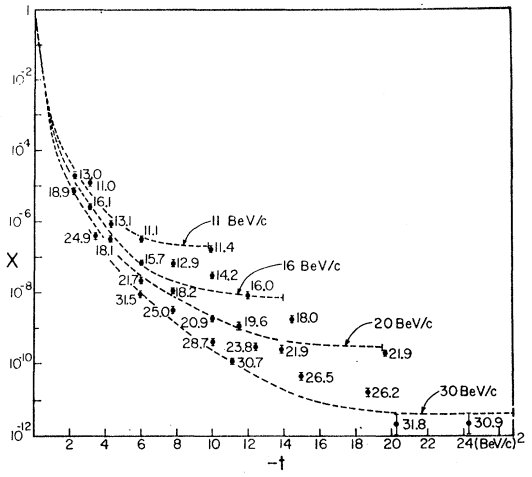

FIG. 7. Elastic differential cross section normalized to the forward scattering cross section, as a function of the squared four-momentum transfer $-t$. Dashed lines describe the behavior of X at fixed beam momenta of 11, 16, 20, and 30 BeV/c; each line ends at t_{max} which corresponds to $\Theta_{c.m.}=90°$.

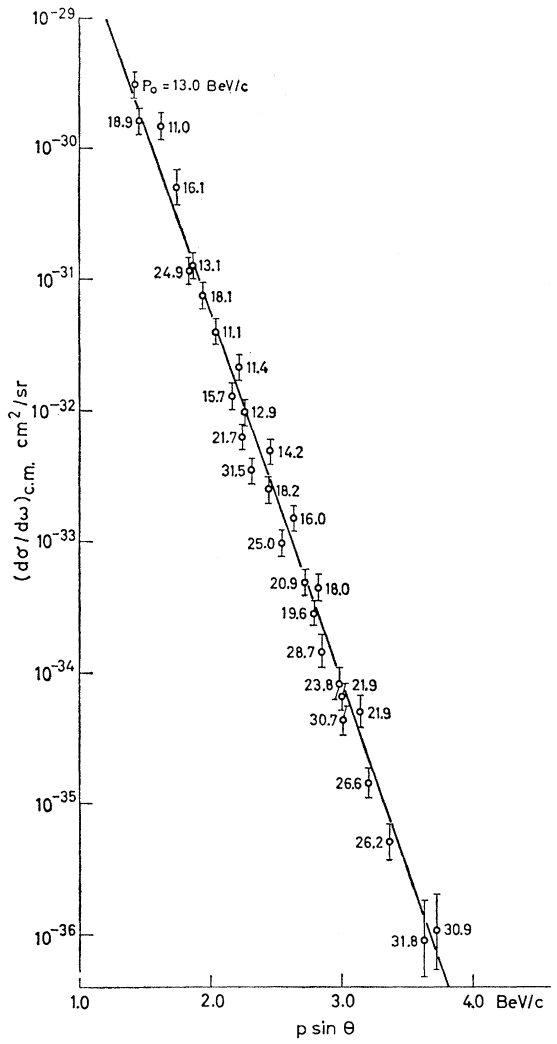

FIG. 8. Plot of the c.m. differential cross sections $(d\sigma/d\omega)_{c.m.}$ as a function of transverse momentum, $p \sin\Theta$. The straight line is $d\sigma/d\omega = A \exp\{-ap_\perp\}$ where $A = 3.0 \times 10^{-26}$ cm^2/sr and $a^{-1} = 152$ MeV/c.

rapidly with increasing momentum transfer than would be expected from the trend of the previous data at lower momentum transfer.

(3) Since $t/t_{max} = (1 - \cos\Theta_{c.m.})$, the curves in Fig. 7 display also the angular distribution for different values of the beam momentum. One can see that all angular distributions are similar in shape. At each momentum the angular distribution becomes practically isotropic (within a factor of 2) for $\Theta_{c.m.}$ between 65 and 90°, i.e., over $\approx 40\%$ of the solid angle. In this region, $(d\sigma/d\omega) \propto e^{a\sqrt{s}}$, where s is the square of the c.m. total energy.

(4) If the data are plotted versus transverse momentum, most of the energy dependence is removed; hence, p-p scattering at high momentum transfer appears to be mainly a function of one variable rather than two.[10,11] This is seen in Fig. 8 where the cross sections are plotted versus $p_\perp = p \sin\Theta$. The fact that the points tend to lie along a straight line is suggestive of some simple type of exponential dependence.[10–12]

Our measurements taken with the results of previous experiments at smaller angles provide a rather complete description of p-p elastic scattering up to the highest energies available with the existing accelerators.

Since the publication in Phys. Rev. Letters (Ref. 3) of our results almost one year ago, many theoretical papers have appeared, where attempts were made at explaining the characteristic features of the p-p elastic cross section. The opinions are divided.

One group of authors[10,13] is inclined to interpret all the p-p elastic scattering as mainly a consequence of diffraction. In fact, by choosing appropriate potentials an optical model can justify the observed features.

Another group of authors,[14] impressed by the exponential dependence of the large angle cross sections upon the c.m. energy, favors a statistical interpretation. The elastic channel is in this case in statistical competition with all inelastic channels, and the observed exponential dependence on c.m. energy is essentially the Boltzmann factor. While a statistical approach can justify the large-angle behavior of the cross section, the angular dependence illustrated by Figs. 7 and 8 remains to be interpreted.

Other theoretical papers have been published that do not fall into the two categories here described.[15]

Further study of the behavior of the inelastic channels and of the large-angle elastic scattering of other particles will help in clarifying the problem.

ACKNOWLEDGMENTS

We wish to thank Dr. J. Hudis for useful discussions and the Be^7 analysis of our many targets. We are grateful to Dr. R. Sugarman of Chronetics Inc. for helpful advice concerning the electronics. We are most indebted to the AGS staff for their invaluable cooperation and help with various special problems of direct concern to this experiment such as the rotating target and the fine control of the flat top.

[10] A. D. Krisch, Phys. Rev. Letters **11**, 217 (1963).

[11] D. S. Narayan and K. V. L. Sarma, Phys. Letters **5**, 365 (1963).

[12] J. Orear, Phys. Rev. Letters **12**, 112 (1964).

[13] R. Serber, Phys. Rev. Letters **10**, 357 (1963); Rev. Mod. Phys. **36**, 649 (1964); and Phys. Rev. Letters **13**, 32 (1964); A. D. Krisch, Phys. Rev. **135**, B1456 (1964); H. H. Aly, D. Lurie, and S. Rosendorff, Phys. Letters **7**, 198 (1963); S. Minami, Phys. Rev. Letters **12**, 200 (1964); and Phys. Rev. **135**, B1263 (1964); H. A. Bethe, Nuovo Cimento **33**, 1167 (1964); A. Baiquni, Phys. Rev. **137**, B1009 (1965); W. N. Cottingham and R. F. Peierls, *ibid.* **137**, B147 (1965). E. M. Henley and I. J. Muzinich, University of Washington preprint (unpublished).

[14] G. Fast and R. Hagedorn, Nuovo Cimento **27**, 203 (1963); G. Fast, R. Hagedorn, and L. W. Jones, *ibid.* **27**, 856 (1963); G. Cocconi, *ibid.* **33**, 643 (1964); L. W. Jones, Phys. Letters **8**, 287 (1964); R. Hagedorn, Nuovo Cimento (to be published); G. Auberson and B. Escoubès, Nuovo Cimento (to be published); A. Bialas and V. Weisskopf, Nuovo Cimento (to be published); J. Vandermeulen, University of Liège (Belgium), preprint, 1964 (unpublished); H. Joos, H. Satz, DESY Hamburg preprint (unpublished).

[15] T. Kinoshita, Phys. Rev. Letters **12**, 257 (1964); K. Yamamoto, Phys. Rev. **134**, B682 (1964), and Enrico Fermi Institute for Nuclear Studies Report 64-11 (unpublished); A. P. Balachandran, Phys. Rev. **137**, B177 (1965), J. Orear, Phys. Letters **13**, 190 (1964); T. T. Wu and C. N. Yang, Phys. Rev. **137**, B708 (1965).